

# Low Resistive TiO<sub>2</sub> Deposition by LPCVD Using TTIP and NbF<sub>5</sub> in Hydrogen-Ambient

Satoshi Yamauchi, Kazuhiro Ishibashi, Sakura Hatakeyama\*

Department of Biomolecular Functional Engineering, Ibaraki University, Hitachi, Japan  
Email: [ysatoshi@mx.ibaraki.ac.jp](mailto:ysatoshi@mx.ibaraki.ac.jp)

Received 27 November 2014; revised 10 December 2014; accepted 2 January 2015

Copyright © 2015 by authors and Scientific Research Publishing Inc.  
This work is licensed under the Creative Commons Attribution International License (CC BY).  
<http://creativecommons.org/licenses/by/4.0/>



Open Access

---

## Abstract

Low resistive TiO<sub>2</sub> layer was deposited by low pressure chemical vapor deposition (LPCVD) at pressure around 0.25 Pa using titanium-tetra-iso-propoxide (TTIP) and NbF<sub>5</sub> in H<sub>2</sub>-ambient. Activation energy for the deposition rate on the temperature was significantly decreased to 120 kJ/mol as compared with 228 kJ/mol for the deposition in H<sub>2</sub> without NbF<sub>5</sub>. The deposition rate linearly increased with NbF<sub>5</sub> supply rate but gradually decreased with H<sub>2</sub> supply rate indicated that F on the deposition surface acts as catalyst for TTIP-dissociation but is non-activated by hydrogen. Resistivity of the layer was decreased by NbF<sub>5</sub> supply depending on the deposition temperature with the activation energy of 319 kJ/mol, whereas the energy was 244 kJ/mol for the layer deposited in H<sub>2</sub> without NbF<sub>5</sub>. The dependence of resistivity on NbF<sub>5</sub> and H<sub>2</sub> supply rates suggested that the doping should be performed by sufficient NbF<sub>5</sub> and H<sub>2</sub> supply rate to improve the crystallinity. As a result of the optimization, the resistivity was successfully reduced to  $5 \times 10^{-2} \Omega\text{-cm}$ . Optical transmission spectra in UV-Vis region indicated that significant absorption observed for the layer deposited in H<sub>2</sub> was notably decreased by using NbF<sub>5</sub>. The improved optical property was better than that for the layer deposited in O<sub>2</sub>-ambient.

## Keywords

LPCVD-TiO<sub>2</sub>, H<sub>2</sub>-Ambient, Nb and F Doping, Low-Resistive TiO<sub>2</sub>, Optical Transmittance

---

## 1. Introduction

It has been well recognized that TiO<sub>2</sub> has interesting properties to fabricate photo-induced applications because of the highly efficient surface photo-catalytic reactions and the hydrophilicity [1] [2]. In addition, the materials can be also used as optoelectronic devices using anti-reflection coating such as solar-cell, optical filter and so on,

---

\*S. Hatakeyama now belongs to Hitachi Industry & Control Solutions, Ltd.

because of the high refractive index [3]. In electronics, TiO<sub>2</sub> with high dielectric constant and relatively high energy band gap was tried to use for gate-dielectrics in MOS-transistor [4], and the semiconductor has been recently expected to be applied for transparent conduction oxide (TCO). For the application as TCO, the anatase-phase is probably more useful than the rutile-phase because energy gap of the anatase (3.2 eV) is wider than that of rutile (3.0 eV) and TiO<sub>2</sub> can be crystallized in anatase-phase at temperature far lower than that required to form rutile-TiO<sub>2</sub>. Further, the conductive TiO<sub>2</sub> with notably high resistance against acid and alkaline solutions has interesting potentials to fabricate wet-type solar-cells such as dye sensitized solar cell [5], chemical sensors etc. However, it is considered that the conductivity control is more difficult than the other TCO such as ITO, Sn<sub>2</sub>O and ZnO since *d*-orbital contributes to forming TiO<sub>2</sub>. Recently, physical vapor deposition such as laser-ablation and reactive sputtering with the post-annealing in reduction ambient have been applied to control the conductivity by using Nb as a donor-dopant and achieved fabrication of highly conductive TiO<sub>2</sub> layer [6] [7]. In the results, it is seemed to be required to enhance the electronic activation of the donor [8], in which Ti<sup>3+</sup> reduced from Ti<sup>4+</sup> probably plays an important role of the conduction in TiO<sub>2</sub>. Although precise control is required to deposit semiconductor layers, chemical vapor deposition (CVD) has great advantages for step coverage on three-dimensional surface. In the CVD process, suitable gas-source as preliminary precursor is fundamentally required with control of the deposition condition. For the deposition of TiO<sub>2</sub> layer, titanium-tetra-iso-propoxide (TTIP:Ti(O-i-C<sub>3</sub>H<sub>7</sub>)<sub>4</sub>) is one of suitable metalorganic precursors. The deposition feature including TTIP-dissociation scheme has been studied on the crystallographic properties, in which it has been recognized that the thermally dissociated species can be crystallized into the anatase-phase around 400°C [9]. However, the conductivity control has not been achieved for TiO<sub>2</sub> layer by CVD. Previously, we demonstrated low pressure chemical vapor deposition (LPCVD) of Nb and F co-doped TiO<sub>2</sub> layer using TTIP and NbF<sub>5</sub> in O<sub>2</sub>-ambient [10], which was resulted in drastic decrease of resistivity to 0.2 Ω·cm in comparison to the resistivity of undoped layer beyond 100 Ω·cm. Here, it was shown by the XPS results that F substituted to the O-site contributes to the reduction of resistivity but CH<sub>x</sub>-F by reaction between alcohol ligands in TTIP and F, in which the fluorination occurred by oxidation of NbF<sub>5</sub>. O<sub>2</sub> gas has been commonly used to deposit anatase-TiO<sub>2</sub> layer by CVD process aiming at reduction of oxygen-deficiency and carbon-impurities; however, the effect for removal carbon impurity is not expected to the deposition using TTIP at such low temperature around 400°C because the precursor is mainly dissociated in the O-R bond of TTIP without oxidation of the alcohol ligands [11]. In contrast, anatase-TiO<sub>2</sub> can be fabricated in H<sub>2</sub> by LPCVD using TTIP as previously reported [12], in which the resistivity was comparably low to Nb and F co-doped layer deposited in O<sub>2</sub> but including structural disordering and significant optical absorptions including Urbach tail in UV-Vis region.

In this paper, LPCVD of TiO<sub>2</sub> layer using TTIP with NbF<sub>5</sub> is demonstrated in H<sub>2</sub>-ambient, and the deposition feature and the resistivity are shown with the optical property in UV-Vis region.

## 2. Experimental

A bell-jar type reactor with the base pressure under  $1 \times 10^{-3}$  Pa by a combination exhaust system consists of a diffusion pump and a rotary pump was used for LPCVD of titanium-oxide. Titanium tetra-iso-propoxide (TTIP, Ti(O-i-C<sub>3</sub>H<sub>7</sub>)<sub>4</sub>: 99.7%-purity) was used as preliminary precursor for the deposition after purification in vacuum. Details of the apparatus configuration and the purification sequence of TTIP were already shown elsewhere [10]. TTIP vaporized from the liquid charge cell at 65°C was introduced into the reactor controlling the supply rate by a variable valve with monitoring the reactor pressure by Schulz gage. In this work, the pressure of TTIP was fixed at  $1.5 \times 10^{-1}$  Pa during TiO<sub>2</sub> deposition. High purity (99.99999%-purity) H<sub>2</sub> gas was also introduced into the reactor through a mass-flow controller calibrated for H<sub>2</sub> gas in ranging from 0.75 to 8.3 sccm, in which the reactor pressure monitored by Schulz gage was varied from  $1.8 \times 10^{-2}$  to  $1.5 \times 10^{-1}$  Pa. TTIP and H<sub>2</sub> were simultaneously introduced into the reactor through individual gas inlets and TiO<sub>2</sub> layer was deposited at pressure ranging from 0.15 to 0.30 Pa. Niobium pentafluoride powder (NbF<sub>5</sub>: 98%-purity) as donor-dopant was charged in a crucible consists of boron-nitride (BN) and then thermally evaporated after purification for 5 hrs in vacuum. Evaporation rate of the dopant was estimated from the total evaporation mass evaluated by an electronic weight scale during the deposition. 1 mm-thick optical-flat quartz plate used as substrate was mounted on a substrate holder after chemical cleaning by organic solvents. Temperature of the substrate holder and the BN crucible were monitored by K-type thermo-couples and controlled by resistive heating with PID-systems using.

Thickness of the layer was checked by a surface profiler (Veeco, DEKTAK150). Resistivity was evaluated by Van Der Pauw (VDP) method using symmetric four ohmic contacts of Indium-dots. UV-Vis optical transmis-

sion spectra were obtained by UV-Vis spectrometer (OCEAN OPTICS: USB-2000) using halogen lamp as a light source.

### 3. Results and Discussion

#### 3.1. Deposition Feature

##### 3.1.1. Dependence of Deposition Rate on the Temperature

**Figure 1** shows deposition rate of undoped layer in H<sub>2</sub>-ambient (black-circle) or O<sub>2</sub>-ambient (open-circle) and Nb-F doped layer (red-circle) in H<sub>2</sub>-ambient at various deposition temperatures in Arrhenius plot, in which the gas flow rate of H<sub>2</sub> or O<sub>2</sub> into the reactor was 4.2 sccm and NbF<sub>5</sub> was evaporated from crucible with the rate about 0.05 mg/min for the deposition of doped layer. Deposition rates of the undoped layers were increased with the temperature and then saturated to the rate about 8 nm/min at the temperature above 360°C, in which the activation energy of 228 kJ/mol in H<sub>2</sub> was clearly larger than that of 138 kJ/mol in O<sub>2</sub>. Here, it is considered that TTIP-dissociation in H<sub>2</sub>-ambient is not owing to chemical reaction on the deposition surface because the higher activation energy is similar to activation barrier of 238 kJ/mol to form Ti(OC<sub>3</sub>H<sub>7</sub>)<sub>3</sub>(OH) through monomolecular dissociation of TTIP calculated by quantum chemical calculations using B3LYP. The surface chemical states have not been identified but it is expected that the surface is terminated by hydroxyls which can be formed during TTIP-dissociation and/or by hydrogenation of oxygen at the surface [12]. On the other, when NbF<sub>5</sub> was simultaneous supplied during the deposition in H<sub>2</sub>, the deposition rate was increased with the activation energy of 120 kJ/mol and then saturated to 18 nm/min above 380°C. The activation energy and the saturation temperature were smaller and higher than that for the undoped layer in H<sub>2</sub>-ambient respectively, which was resulted in higher saturated deposition rate. The results clearly indicate TTIP-dissociation in H<sub>2</sub> was promoted by NbF<sub>5</sub>. Here, it is difficult to recognize reduction of the activation energy by NbF<sub>5</sub> supply in H<sub>2</sub> is due to fluorination of TTIP because the fluorination reduces the deposition rate as shown previously for the deposition in O<sub>2</sub>-ambient [10]. Further, it is mentioned sticking probability of TTIP on the deposition surface was increased by NbF<sub>5</sub> contribution because the saturated deposition rate at high temperature was increased by NbF<sub>5</sub> supply. As the results, it should be concluded that the TTIP-dissociation was promoted by reactive site on the surface contributed by NbF<sub>5</sub>.

##### 3.1.2. Dependence of Deposition Rate on NbF<sub>5</sub> & H<sub>2</sub> Supply Rate

Deposition feature of the doped layer was also influenced by NbF<sub>5</sub> and H<sub>2</sub> gas supply rate. **Figure 2(a)** shows dependence of TiO<sub>2</sub> deposition rate at 380°C in H<sub>2</sub> with the flow rate of 0.75 (open-circle), 4.2 (solid-circle) and 8.3 sccm (solid-triangle) on NbF<sub>5</sub> evaporation rate from crucible, where TTIP supply rate was same for the depositions. The deposition rate was linearly increased and then gently decreased with NbF<sub>5</sub> evaporation rate de-

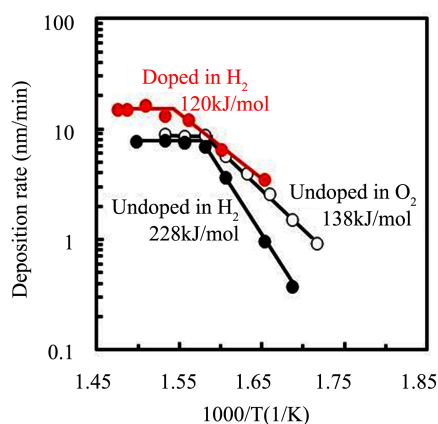


**Figure 1.** Deposition rate of undoped (black-circle) and Nb-F doped (red-circle) layers in H<sub>2</sub>-ambient and undoped layers in O<sub>2</sub>-ambient (open-circle) at various deposition temperatures, where the layers were deposited at 0.25 Pa with H<sub>2</sub> or O<sub>2</sub> flow rate of 4.2 sccm. NbF<sub>5</sub> was evaporated with the rate about 0.05 mg/min for the deposition of doped layer.

pending on  $H_2$  flow rate. It is easily expected that F play an important role for TTIP-dissociation but not the fluorination. Further, it is difficult to recognize that the significant increase of deposition rate was due to the reaction between TTIP and F in vapor phase because the density of  $NbF_5$  was far lower than the TTIP, in which the  $NbF_5$ /TTIP supply ratio can be roughly estimated as a few % from the  $TiO_2$  deposition rate and the  $NbF_5$  evaporation rate with taking the reactor structure into account. Therefore, it should be discussed the TTIP-dissociation contributed by F on the deposition surface as shown in the next section. It is however considered the excessive  $NbF_5$  fluorinates TTIP, which is resulted in decrease of the deposition rate. Since structural disordering in the layer is enhanced by the fluorination of alcohol ligands of TTIP as previously suggested [10], the excess  $NbF_5$ -supply on the deposition surface is insufficient for the deposition. The deposition rate linearly increased with  $NbF_5$  evaporation rate was decreased with  $H_2$  flow rate as shown in **Figure 2(b)**, in which incremental rate of deposition rate due to  $NbF_5$  evaporation rate is shown for  $H_2$  flow rate. The result suggested density of the reactive species for TTIP-dissociation on the deposition surface is decreased with  $H_2$  density on the surface, which can be recognized that surface F is non-activated as HF by H.

### 3.1.3. Expected Deposition Scheme on Deposition Surface

Previously, it was reported that HF interacts to hydroxyl groups and oxygen on  $TiO_2$  surface by hydrogen-bonding in weak acidic HF solution and hydroxyl groups on  $TiO_2$  surface is easily exchanged to F in strong acidic HF solution [13]. Although HF is not preliminary supplied on the deposition surface in the LPCVD process, it is expected that Ti-F is formed with  $NbF_4OH$  by the reaction between  $NbF_5$  and hydroxyls on the surface, then HF is produced after TTIP is adsorbed at the reactive site of surface F in Ti-F. According to the reaction, a possible scheme for the deposition with  $NbF_5$ -supply can be depicted in **Figure 3**. When  $NbF_5$  is supplied on surface hydroxyl groups in **Scheme 1**, the OH is exchanged to F with formation of  $NbF_4OH$  (**Scheme 2**). The next coming TTIP adsorbed to the surface F is dissociated with forming HF and propene, and then the partially dissociated TTIP is coordinated to surface Ti (**Scheme 2** & **Scheme 4**) as O-Ti-(OR)<sub>3</sub> which then form oxo-bridging between the neighbors via the thermal dissociation. Here, the produced HF interacts to the neighbor hydroxyl groups ( $\equiv Ti-OH$ ) and oxygen (Ti-O) (**Scheme 4**), then  $\equiv Ti-F$  is formed with product of  $H_2O$  (**Scheme 5**), in which the reactions from **Scheme 2** to **Scheme 5** are sequentially processed on the deposition surface. As previously discussed, TTIP-dissociation is owing to the monomolecular thermal process due to the low sticking probability on the hydrogen-terminated surface (**Scheme 1**), which is resulted in the significant increased activation energy for the deposition rate in  $H_2$ -ambient [12]. In contrast, it is expected the surface F with high electron negativity acts as catalyst for partial dissociation of TTIP (from **Scheme 3** to **Scheme 4**). As the result, activation energy for the deposition rate is significantly decreased by  $NbF_5$ -supply as shown in **Figure 1** and the deposition rate is increased with the density of F ( $NbF_5$  evaporation rate) as shown in **Figure 2(a)**, whereas the of F-density is far lower than that of TTIP. It is noted that hydrogen supplied as  $H_2$  gas acts to form HF on the surface before TTIP is adsorbed to the surface F in **Scheme 2** or **Scheme 5**, which is resulted in decrease

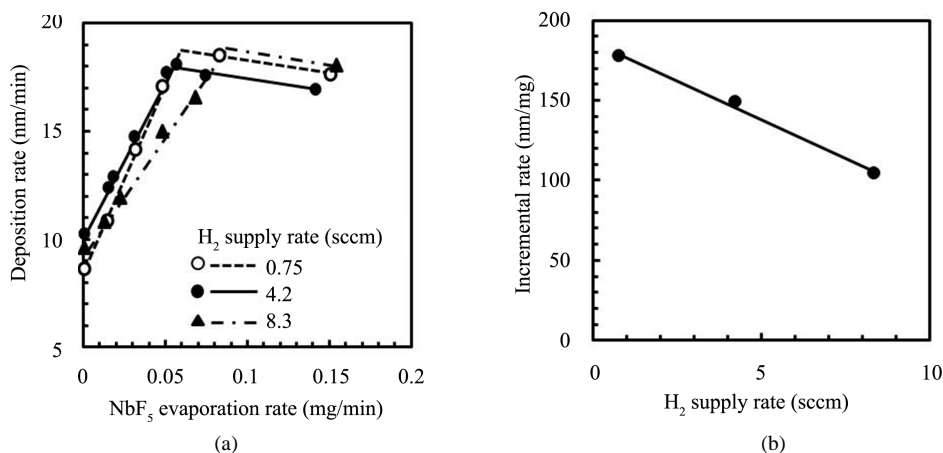


**Figure 2.** (a) Dependence of deposition rate on  $NbF_5$  evaporation rate in  $H_2$  flow rate of 0.75 (solid-circle), 4.2 (open-circle) and 8.3 sccm (solid-triangle); (b) Dependence of incremental rate for deposition rate by  $NbF_5$  in the evaporation rate below 0.05 mg/min on  $H_2$  flow rate.

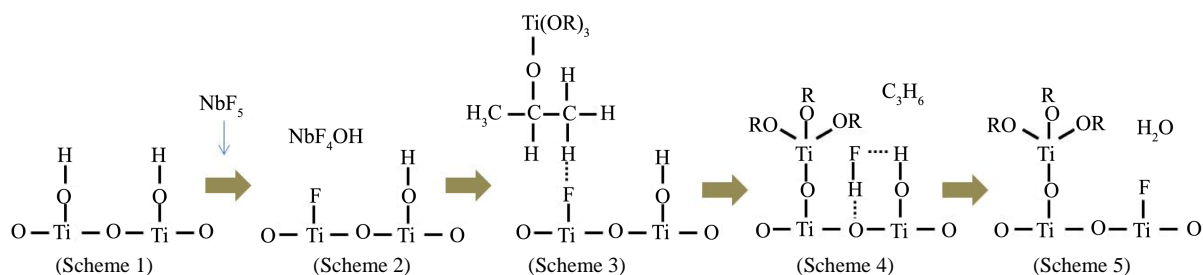


**Figure 3.** An expected dissociation scheme for TTIP and  $\text{NbF}_5$ .

of the deposition rate with increasing the  $\text{H}_2$  flow rate as shown in **Figure 2(b)**. On the other, excessively supplied  $\text{NbF}_5$  probably causes fluorination of alcohol ligands in **Scheme 4** or **Scheme 5**, which is insufficient to control property of the layer because significant structural disordering is introduced into the layer.

## 3.2. Electric Property

### 3.2.1. Dependence of Resistivity on Deposition Temperature

**Figure 4** shows resistivity of undoped (black-circle) and doped (red-circle) layers with the thickness about 200 nm deposited at various temperatures in  $\text{H}_2$  with the flow rate of 4.2 sccm, where  $\text{NbF}_5$  evaporation rate was fixed at 0.05 mg/min for the doping. Resistivity of the undoped layer was decreased with increasing the deposition temperature according to the activation energy of 244 kJ/mol but increased beyond  $360^\circ\text{C}$ . In case of the doped layer, the resistivity higher than the undoped layer at low temperature was also decreased with the deposition temperature below  $380^\circ\text{C}$  with larger activation energy (319 kJ/mol) than the undoped layer. As the result, resistivity of the doped layer deposited at temperature beyond  $370^\circ\text{C}$  was more reduced than the undoped layer. We previously speculated that  $\text{Ti}^{3+}$  is formed in the layer with oxygen-vacancy by desorption of hydrogen from  $\text{H-Ti}\equiv$  formed in  $\text{H}_2$ -ambient, in which the resistivity is decreased with the temperature according to the dissociation energy of  $\text{H-Ti}\equiv$  [12]. It is however difficult the same scheme for the layer deposited by  $\text{NbF}_5$  supply in  $\text{H}_2$  because the activation energy was larger than the dissociation energy. When  $\text{NbF}_5$  is simultaneously supplied to the deposition surface, F and Nb substituted to O-site and Ti-site are expected to act as relatively shallow donors in  $\text{TiO}_2$  respectively, where the F generates  $\text{Ti}^{3+}$  without O-vacancies and the  $\text{Ti}^{3+}$  forms  $\text{Ti-}3d^1$  band [14]. In contrast, interstitial F and anti-site Nb reduce the carrier density because such defects act as acceptors. In case of the doping in  $\text{O}_2$ -ambient, F is substituted to the O-site but the crystallinity was significant degraded by fluorination of TTIP due to oxidation of  $\text{NbF}_5$  [10]. In contrast, it is considered the fluorination can be prevented in  $\text{H}_2$ -ambient because of removal the oxidant for  $\text{NbF}_5$  but Nb reduced from  $\text{NbF}_5$  by hydrogen maybe substitute the O-site. Indeed, the activation energy of 319 kJ/mol is close to the bond dissociation energy of Nb-Ti (302 kJ/mol) [15]. On the other, the resistivity was increased at high temperature beyond  $360^\circ\text{C}$  for the undoped layer and  $380^\circ\text{C}$  for the doped layer. It is interesting the deposition rate was limited by TTIP-supply rate at such high temperatures, which indicates the most efficient doping can be achieved at the highest temperature in surface reaction limited region for the deposition rate.

### 3.2.2. Dependence on $\text{NbF}_5$ & $\text{H}_2$ Supply Rate

**Figure 5(a)** shows resistivity of the layer as a function of  $\text{NbF}_5$  evaporation rate in  $\text{H}_2$  with the flow rate of 0.75 (open-circle), 4.2 (solid-circle) and 8.3 sccm (solid-triangle), where the layers were deposited with the thickness about 200 nm at  $380^\circ\text{C}$ . The results can be recognized not only  $\text{NbF}_5$  evaporation rate but also  $\text{H}_2$  flow rate affects to the doping feature. For the  $\text{NbF}_5$  evaporation rate, the resistivity was decreased with increasing the evaporation rate but the feature was different in the high evaporation rate. Since the deposition feature was disturbed in the high  $\text{NbF}_5$  evaporation rate as shown in **Figure 2(a)**, it is not easy to discuss the dependence of resistivity on the doping in the high  $\text{NbF}_5$  evaporation rate. In contrast, the resistivity in the low  $\text{NbF}_5$  evaporation rate is uniquely decreased with the evaporation rate, where the dependence should be discussed for  $\text{NbF}_5$  density on the deposition surface. The  $\text{NbF}_5$  supply rate on the deposition surface ( $\mu_{\text{NbF}_5}$ ) is proportional to  $[\text{NbF}_5]/\text{DR}$ , because the density is increased with  $\text{NbF}_5$  evaporation rate ( $[\text{NbF}_5]$ ) and decreased with deposition rate of the layer (DR). **Figure 5(b)** shows resistivity of the doped layer for  $[\text{NbF}_5]/\text{DR}$  in log-log scale. Resistivity of the doped layer ( $\rho_{\text{doped}}$ ) was decreased with  $[\text{NbF}_5]/\text{DR}$ , which was resulted in the relationship of  $\rho_{\text{doped}} \sim (\mu_{\text{NbF}_5})^n$ . If

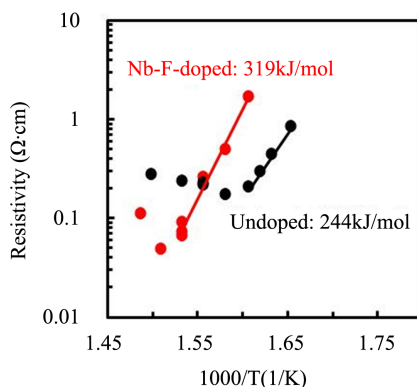


**Figure 4.** Resistivity of undoped (black-circle) and Nb-F doped (red-circle) layers in  $H_2$ -ambient at various deposition temperatures, where the resistivity was evaluated for the layers with the thickness about 200 nm.

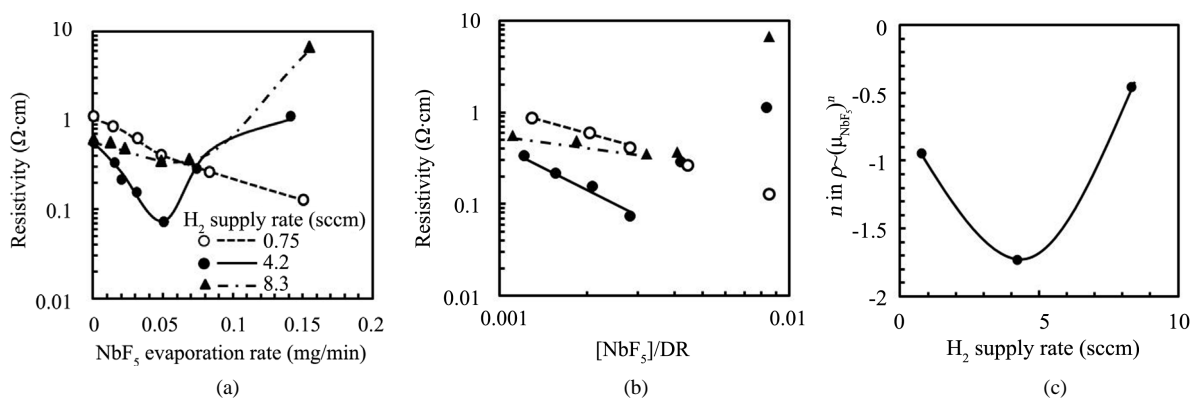


**Figure 5.** Variation of  $TiO_2$  layer resistivity for (a)  $NbF_5$  evaporation rate and (b)  $[NbF_5]/DR$  in  $H_2$  with the flow rate of 0.75 (open-circle), 4.2 (solid-circle) and 8.3 sccm (solid-triangle), where  $[NbF_5]$  and  $DR$  is  $NbF_5$  evaporation rate and deposition rate of layer respectively, and (c) dependence of  $n$ -factor in a relationship of  $\rho_{doped} \sim (\mu_{NbF_5})^n$ , where  $\rho_{doped}$  and  $\mu_{NbF_5}$  is resistivity of doped layer and  $NbF_5$  density on the deposition surface on  $H_2$  flow rate.

the donor was simply increased in the density with  $\mu_{NbF_5}$ , the resistivity should be decreased in the factor  $n$  of  $-1$ . In contrast, the factor  $n$  less than  $-1$  and beyond  $-1$  suggests the crystallinity including the grain boundary was improved and degraded with the donor density, respectively. In the result of **Figure 5(b)**, the factor for the deposition in  $H_2$  with the flow rate of 0.75, 4.2 and 8.3 sccm was  $-0.94$ ,  $-1.7$  and  $-0.45$  respectively. **Figure 5(c)** shows variation of the factor  $n$  for the  $H_2$  flow rate, in which the factor  $n$  was decreased with the  $H_2$  flow rate but notably increased by excess  $H_2$  flow rate. It should be mentioned here that the factor  $n$  was less than  $-1$  for the deposition with  $H_2$  supply rate of 4.2 sccm. The interesting result suggests the doping with sufficient  $H_2$  supply not only increased donor density but also improved the crystallinity. In previous report, we speculated oxygen-vacancies increase resistivity of the doped layer [10], in which the defects probably form complex centers with deep levels. In contrast, it is expected that F doping into O-site in  $TiO_2$  achieves to reduce the O-vacancies in the density and creates  $Ti^{3+}$  with shallow donor level. Of course, the doping feature is owing to the dissociation scheme of the dopant. The result of the factor  $n$  dependent on  $H_2$  flow rate indicates sufficient hydrogen supply is required for the efficient doping but excess hydrogen is resulted in invalidation of the doping. The insufficient doping in excess  $H_2$  is probably caused by anti-site Nb which is introduced by species excessively reduced from  $NbF_5$  as speculated in the Section 3.1.1.

### 3.2.3. Optical Property

**Figure 6(a)** shows transmission spectra in UV-Vis region of undoped layer (black-line) and Nb-F doped layer (red-line) deposited in  $H_2$ , in addition to the spectrum of Nb-F doped layer deposited in  $O_2$  (blue-line) [9]. The layers were deposited with the thickness about 200 nm by the condition optimized to reduce the resistivity and

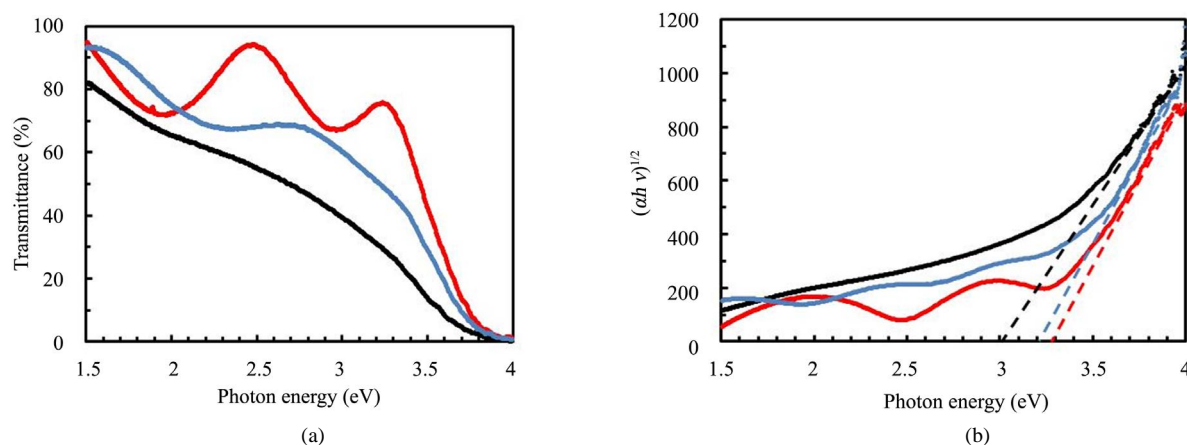


**Figure 6.** (a) Transmission spectra and (b) the Tauc-plot in  $(\alpha h\nu)^{1/2}$  vs. photon energy of undoped layer (black-line) and Nb-F doped layer (red-line) deposited in  $H_2$ , and Nb-F doped layer (blue-line) deposited in  $O_2$ , where the layers were deposited with the thickness about 200 nm by the optimized conditions.

resulted in the resistivity of 0.2, 0.05 and 0.2  $\Omega\cdot\text{cm}$  for the undoped and the Nb-F doped layers in  $H_2$  and the Nb-F doped layer in  $O_2$  respectively. Here, the spectrum of undoped layer in  $O_2$  was similar to the blue line. As previously reported, the undoped layer in  $H_2$  showed broad optical-absorptions around 3.0 eV and 2.2 eV due to deep levels concerned with oxygen-vacancies and  $Ti^{3+}$  [10] respectively. In contrast, although significant multi-reflection was included, such absorptions were remarkably prevented in the spectrum of the doped layer deposited in  $H_2$ . Especially, the absorption around 3.0 eV was obviously decreased in the doped-layer, which indicated density of oxygen-vacancy in the doped layer was notably reduced in comparison to the undoped layer. It is not difficult to anticipate O-vacancy is easily induced into the oxide in  $H_2$ -ambient but is not originated from the reduction of  $TiO_2$  in the CVD-process. The defect is probably formed by TTIP-dissociation via monomolecular thermal dissociation as suggested previously [12]. In the case of simultaneous supply of  $NbF_5$ , the dissociation scheme is quite differed as shown in Figure 3, in which TTIP can be chemically dissociated at the reactive site of F on the deposition surface. As the result, the deposition can be performed with preventing O-vacancy by the dissociation supported by the surface F. In addition, F-doping into the O-site may reduce the density of O-vacancy. It is noted that the optical transparency of the Nb-F doped layer deposited in  $H_2$  was better than the doped layer in  $O_2$ . Commonly,  $O_2$ -gas has been used for CVD of  $TiO_2$  to improve the property aiming at removal oxygen-deficiency and residual carbon-related impurities. However, the results for optical absorption revealed  $H_2$  simultaneously supplied with  $NbF_5$  is more effective than  $O_2$  to reduce optical absorption due to deep-levels especially originated from oxygen-vacancies. It is believed the reduction of the deep-level density was come from the sufficient TTIP-dissociation on the deposition surface and F substituted to the oxygen-site. On the other, structural disordering causes the optical band gap narrowing due to absorption tail below the fundamental absorption edge which is referred as Urbach tail [16]. Figure 6(b) is Tauc-plot in  $(\alpha h\nu)^{1/2}$  vs. photon energy, where  $\alpha$ ,  $h$  and  $\nu$  is absorption coefficient, Plank constant and wavenumber respectively. Optical band gap of 3.0 eV for the undoped layer in  $H_2$  was narrower than 3.2 eV for anatase- $TiO_2$ . In contrast, the band gap energy of 3.27 eV for the doped layer was in good agreement with 3.26 eV for anatase- $TiO_2$  [17], which indicated structural disordering in the doped layer was significantly improved as compared with in the undoped layer. Here, the band gap energy of 3.20 eV for the doped layer in  $O_2$  was slightly large as compared with the energy of 3.16 eV for the undoped layer in  $O_2$  [12], which suggested the structural disordering can be improved also in  $O_2$  by  $NbF_5$ -supply. However, the larger energy of 3.26 eV for the doped layer in  $H_2$  indicated  $NbF_5$ -supply in  $H_2$  is more effective than that in  $O_2$ .

#### 4. Conclusion

Low-pressure chemical vapor deposition of  $TiO_2$  layer was demonstrated in  $H_2$ -ambient by using TTIP with  $NbF_5$ . Activation energy for the deposition rate was significantly reduced to 120 kJ/mol by  $NbF_5$ -supply in comparison to the energy as high as 228 kJ/mol for the deposition without  $NbF_5$ . In addition, the deposition limited by the surface reaction of TTIP was performed at temperature below 380°C, whereas the deposition with-

out NbF<sub>5</sub>-supply above 360°C was limited by the TTIP-supply rate. The deposition rate at 380°C was linearly increased with NbF<sub>5</sub>-supply rate but slightly decreased by the excess supply. An expected scheme for TTIP and NbF<sub>5</sub> dissociation suggested that F dissociated from NbF<sub>5</sub> by reaction between NbF<sub>5</sub> and OH on the deposition surface acts as catalyst for TTIP. Resistivity of the layer was decreased with increasing deposition temperature in the surface reaction limited region for the deposition rate, in which the activation energy of 319 kJ/mol is higher than 244 kJ/mol for the layer deposited without NbF<sub>5</sub>. The results for resistivity dependent on NbF<sub>5</sub> and H<sub>2</sub> supply rates indicated that H<sub>2</sub> is required to achieve efficient doping but excess H<sub>2</sub> increases the resistivity. As the result, TiO<sub>2</sub> layer with the resistivity as low as  $5 \times 10^{-2} \Omega\text{-cm}$  could be fabricated by LPCVD using TTIP and NbF<sub>5</sub> in H<sub>2</sub>-ambient. Further, optical transmission spectra showed that the density of optical absorption centers in UV-Vis region was notably decreased in the low resistive layer deposited in H<sub>2</sub> with NbF<sub>5</sub>-supply as compared with the undoped layer and the Nb-F doped layer in O<sub>2</sub>, in addition to increase of the optical absorption edge energy. Such results clearly indicated that low-resistive TiO<sub>2</sub> layer with high transparency can be deposited by the presented process using TTIP with NbF<sub>5</sub> in H<sub>2</sub>-ambient.

## References

- [1] Wang, R., Hashimoto, K. and Fujishima, A. (1997) Light-Induced Amphiphilic Surfaces. *Nature*, **388**, 431-432. <http://dx.doi.org/10.1038/41233>
- [2] Mills, A., Lepre, A., Elliott, N., Bhopal, A., Parkin, I.P. and Neill, S.A. (2003) Characterisation of the Photocatalyst Pilkington Activ™: A Reference Film Photocatalyst? *Journal of Photochemistry and Photobiology A: Chemistry*, **160**, 213-224. [http://dx.doi.org/10.1016/S1010-6030\(03\)00205-3](http://dx.doi.org/10.1016/S1010-6030(03)00205-3)
- [3] Martinet, C., Paillard, V., Gagnaire, A. and Joseph, J. (1997) Deposition of SiO<sub>2</sub> and TiO<sub>2</sub> Thin Films by Plasma Enhanced Chemical Vapor Deposition for Antireflection Coating. *Journal of Non-Crystalline Solids*, **216**, 77-82. [http://dx.doi.org/10.1016/S0022-3093\(97\)00175-0](http://dx.doi.org/10.1016/S0022-3093(97)00175-0)
- [4] Campbell, S.A., Kim, H.S., Gilmer, D.C., He, B., Ma, T. and Gladfelter, W.L. (1999) Titanium Dioxide (TiO<sub>2</sub>)-Based Gate Insulators. *IBM Journal of Research and Development*, **43**, 383-392. <http://dx.doi.org/10.1147/rd.433.0383>
- [5] O'Regan, B. and Grätzel, M. (1991) A Low-Cost, High-Efficiency Solar Cell Based on Dye-Sensitized Colloidal TiO<sub>2</sub> Films. *Nature*, **353**, 737-740. <http://dx.doi.org/10.1038/353737a0>
- [6] Hitosugi, T., Ueda, A., Furubayashi, Y., Hirose, Y., Konuma, S., Shimada, T. and Hasegawa, T. (2006) Fabrication of TiO<sub>2</sub>-Based Transparent Conducting Oxide Films on Glass by Pulsed Laser Deposition. *Japanese Journal of Applied Physics*, **46**, L86-L88. <http://dx.doi.org/10.1143/JJAP.46.L86>
- [7] Gillispie, M.A., van Hest, M.F.A.M., Dabney, M.S., Perkins, J.D. and Ginley, D.S. (2007) rf Magnetron Sputter Deposition of Transparent Conducting Nb-Doped TiO<sub>2</sub> Films on SrTiO<sub>3</sub>. *Journal of Applied Physics*, **101**, Article ID: 033125. <http://dx.doi.org/10.1063/1.2434005>
- [8] Hoang, N.L., Yamada, N., Hitosugi, T., Kasai, J., Nakao, S., Shimada, T. and Hasegawa, T. (2008) Low-Temperature Fabrication of Transparent Conducting Anatase Nb-Doped TiO<sub>2</sub> Films by Sputtering. *Applied Physics Express*, **1**, 115001-115003. <http://dx.doi.org/10.1143/APEX.1.115001>
- [9] Zhang, A. and Griffin, L. (1995) Gas-Phase Kinetics for TiO<sub>2</sub>: Hot-Wall Reactor Results. *Thin Solid Films*, **263**, 65-71. [http://dx.doi.org/10.1016/0040-6090\(95\)06580-6](http://dx.doi.org/10.1016/0040-6090(95)06580-6)
- [10] Yamauchi, S., Saiki, S., Ishibashi, K., Nakagawa, A. and Hatakeyama, S. (2014) Low Pressure Chemical Vapor Deposition of Nb and F Co-Doped TiO<sub>2</sub> Layer. *Journal of Crystallization Process and Technology*, **4**, 79-88. <http://dx.doi.org/10.4236/jcpt.2014.42011>
- [11] Gao, Y., Perkins, C.L., He, S., Alluri, P., Tran, T., Thevuthasan, S. and Henderson, M.A. (2000) Mechanistic Study of Metalorganic Chemical Vapor Deposition of (Ba, Sr)TiO<sub>3</sub> Thin Films. *Journal of Applied Physics*, **87**, 7430-7437. <http://dx.doi.org/10.1063/1.373005>
- [12] Yamauchi, S., Ishibashi, K. and Hatakeyama, S. (2014) Low Pressure Chemical Vapor Deposition of TiO<sub>2</sub> Layer in Hydrogen-Ambient. *Journal of Crystallization Process and Technology*, **4**, 185-192. <http://dx.doi.org/10.4236/jcpt.2014.44023>
- [13] Liu, S., Yu, J., Cheng, B. and Jaroniec, M. (2012) Fluorinated Semiconductor Photocatalysts: Tunable Synthesis and Unique Properties. *Advances in Colloid and Interface Science*, **173**, 35-53. <http://dx.doi.org/10.1016/j.cis.2012.02.004>
- [14] Valentin, C.D., Pacchioni, G. and Selloni, A. (2009) Reduced and n-Type Doped TiO<sub>2</sub>: Nature of Ti<sup>3+</sup> Species. *The Journal of Physical Chemistry C*, **113**, 20543-20552. <http://dx.doi.org/10.1021/jp9061797>
- [15] Ride, D.R. (2005) CRC Handbook of Chemistry and Physics. CRC Press, LLC, Boca Raton.
- [16] Urbach, F. (1953) The Long-Wavelength Edge of Photographic Sensitivity and of the Electronic Absorption of Solids.

*Physical Review*, **92**, 1324. <http://dx.doi.org/10.1103/PhysRev.92.1324>

- [17] Tsukada, M., Wakamura, M., Yoshida, N. and Watanabe, T. (2011) Band Gap and Photocatalytic Properties of Ti-Substituted Hydroxyapatite: Comparison with Anatase-TiO<sub>2</sub>. *Journal of Molecular Catalysis A: Chemical*, **338**, 18-23. <http://dx.doi.org/10.1016/j.molcata.2011.01.017>

Scientific Research Publishing (SCIRP) is one of the largest Open Access journal publishers. It is currently publishing more than 200 open access, online, peer-reviewed journals covering a wide range of academic disciplines. SCIRP serves the worldwide academic communities and contributes to the progress and application of science with its publication.

Other selected journals from SCIRP are listed as below. Submit your manuscript to us via either [submit@scirp.org](mailto:submit@scirp.org) or [Online Submission Portal](#).

